Random Motility of Swimming Bacteria: Single Cells Compared to Cell Populations

Bret R. Phillips and John A. Quinn
Dept. of Chemical Engineering, University of Pennsylvania, Philadelphia, PA 19104

Howard Goldfine
Dept. of Microbiology, School of Medicine, University of Pennsylvania, Philadelphia, PA 19104

The motility of a population of swimming bacteria can be characterized by a random motility coefficient, μ, the operational equivalent of a diffusion coefficient at the macroscopic level and in the absence of interacting chemical gradients. At the microscopic level, random motility is related to the single-cell parameters: speed, tumbling probability, and index of directional persistence (related to the angle a cell's path assumes following a change in direction). Various mathematical models have been proposed for relating the macroscopic random motility coefficient to these microscopic single-cell parameters. In separate experiments, we have measured motility at both the cell-population and single-cell levels for Escherichia coli. *The agreement of these results shows that the macroscopic transport behavior of a population of motile bacteria can be predicted from straightforward microscopic observations on single cells.*

Introduction

A characteristic feature of many motile microorganisms is their zigzag movement which may be represented approximately as a sequence of straight line steps interrupted by turns (Hall, 1977). The swimming motion of the bacterium *Escherichia coli* illustrates this behavior. *E. coli* swim in a series of smooth straight paths called "runs" which are terminated by a rapid turning maneuver called a "tumble." This gives the cell a nearly random reorientation from which to begin the next run (Berg and Brown, 1972). This run and tumble random motility behavior can best be approximated as a three-dimensional random walk. In the presence of a spatial or temporal gradient of an attractant (sugars and amino acids), a bacterium swimming up the gradient will suppress its tumbling response. This results in a longer run in the direction of the higher attractant concentration (Brown and Berg, 1974; Macnab and Koshland, 1972; Lovely et al., 1974; Tsang et al., 1973); the opposite response, that is, a longer run in the direction of lower concentration is displayed in the presence of a repellent (pH extremes and aliphatic alcohols). This behavior, termed chemoklinokinesis, enables an individual bacterium to control its tumbling frequency, and results in a biased or directed random walk towards attractants and away from repellents. At the macroscopic cell-population level, this net migration is termed chemotaxis. This behavior is illustrated in Figure 1.

The bacterium *E. coli* is a peritrichously (uniformly) flagellated, rod-shaped organism approximately 2 μm long and 1 μm in diameter. *E. coli* has on average eight flagellar filaments, each $\approx$5-10 μm long and 20 nm in diameter (O'Brien and Bennett, 1972). Motility is generated by a reversible rotary motor located at the base of each flagellar filament (Berg and Anderson, 1973; Silverman and Simon, 1974). When rotated in the counterclockwise direction (as viewed from the distal end), the flagella form a coordinated bundle which propels the cell, resulting in the run type behavior discussed above. A clockwise rotation of the flagellum results in a disruption of the coordinated bundle which causes the cell to move chaotically or tumble (Larsen et al., 1974; Macnab and Ornston, 1977). Due to the random-walk behavior of individual cells, the dispersion of a population of cells in an isotropic medium can be described in terms of a random motility coefficient, μ, the operational equivalent of a diffusion coefficient. For a single cell, motility can be further interpreted in terms of its speed, s, tumbling frequency (or the reciprocal mean run length

Correspondence concerning this article should be addressed to J. A. Quinn. Current address of B. R. Phillips: Merck & Co., Inc., Danville, PA.

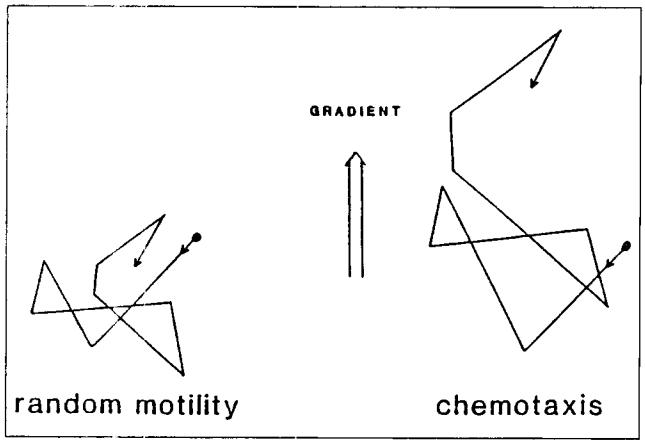

Figure 1. Bacterial motility in absence and presence of a chemical gradient.

Left: random motility in which the cell alternately swims and tumbles. Tumbles occur with constant probability (Poisson statistics) and give the cell a nearly random reorientation to begin the next run (see Results and Discussion). Right: biased motility or chemotaxis, in which the tumbling probability is decreased when the cell is swimming toward higher attractant/lower repellent concentration (Macnab, 1979).

time), λ_T, and the index of directional persistence, ψ_d (Othmer et al., 1988). Speed is defined as the cell's linear velocity during a run. Run length time (or run displacement divided by velocity) can be defined as the time between tumbles; due to the Poisson nature of the underlying random processes, the inverse mean run length time is equivalent to the tumbling frequency or the tumbling probability. The index of directional persistence is related to the turn angle, that is, the angle between consecutive runs.

Bacterial motility is a dominant factor in a number of microbial processes. It has been shown to play important rolls in both nitrogen fixation—the incorporation of atmospheric nitrogen in plant culture, and denitrification—the reduction of nitrate or nitrite to nitrous oxide or elemental nitrogen (Armitage et al., 1988; Gulash et al., 1984; Kennedy and Lawless, 1985). Evidence exists suggesting that motility may be one of the mechanisms that controls bacterial interactions with the mammalian gastrointestinal tract (Aldweiss et al., 1977; Freter et al., 1981; Stanton and Savage, 1983). Chet and coworkers (1975) found that motility can be used to control biofilm formation. Bacterial motility is also a vital aspect of many bioremediation technologies. Successful bioremediation may require that biodegradable bacteria move through soil, aquifer solids or groundwater (Gannon et al., 1991). It is clear that a quantitative characterization of bacterial motility is necessary in order to fully understand both naturally occurring microbial transport and current biotechnological applications.

We have found few reports of quantitative measurements of motility parameters at either the macroscopic cell-population or microscopic single-cell levels. At the cell-population level, less than a dozen measurements of a random motility coefficient have been reported. At the microscopic level, the paths of individual swimming cells have been followed by the ingenious three-dimensional tracking microscope first develped by Berg and coworkers (Berg, 1971; Berg and Brown, 1972; Brown and Berg, 1974; Lovely et al., 1974; Lowe et al., 1987). Other researchers (Maeda et al., 1976; Macnab and Koshland, 1972; Schneider and Doetsch, 1974; Poole et al., 1988; Taylor and Koshland, 1975) have used photography and cinematography to investigate single-cell motility. The results of these investigations in relation to those presented here are discussed in the Results and Discussion section of this article. For a more detailed discussion of motility assays see Ford et al. (1991).

Because the random motility of the cell population as a whole is the result of the swimming behavior of each noninteracting individual cell, the two are fundamentally related. Furthermore, because the net motion of single cells can be modeled with three independent parameters, they provide a basis for describing the transport of the cell population. The theoretical models of Othmer et al. (1988) and Rivero et al. (1989) relate microscopic single-cell parameters to the macroscopic random motility coefficient. These models were tested by Farrell et al. (1990) who investigated the two-dimensional migration of alveolar macrophages, but they have not been rigorously applied to bacteria swimming in three dimensions.

In this article we present the results of experiments in which motility parameters for *E. coli* AW405 have been measured at both the macroscopic cell-population and microscopic single-cell levels. Motility measurements were also gathered for cells swimming in the presence of two different uniform concentrations of serine, an amino acid known to effect the motility of this strain (Berg and Brown, 1972). For the macroscopic measurements, a stopped-flow diffusion cell was used to establish an initial step gradient in cell concentration which decayed over time. At distinct time intervals, bacterial spatial distributions were recorded photographically. Computer-aided image analysis of the photographic negatives yielded the actual bacterial concentration profiles. From concentration profiles a random motility coefficient could be calculated. Ford et al. (1991) reported preliminary investigations using this same procedure. This approach has proven to be a reliable and precise method for measuring the random motility of a cell population. In comparison to the commonly used capillary assay, the method presented here can be shown to be a more precise and versatile approach. For the microscopic measurements, computer-aided image analysis was used to measure single-cell parameters (speed and run length time) from a video recording of swimming cells. Since this method did not easily allow direct measurement of the turn angle, we were unable to directly measure the index of directional persistence, ψ_d. However, by comparing these measured values of motility parameters at both the cell population and single-cell levels with the theoretical models relating the two, the index of directional persistence, ψ_d, was determined. Prior to this investigation, the only reported measurements of ψ_d for bacteria were obtained using a tracking microscope; the values measured here compare well with those measurements.

The following section contains descriptions of two novel experimental procedures which were used in the measurement of motility parameters at the cell-population and single-cell levels. The data obtained are then compared with a mathematical model relating the two. Finally, these results are discussed in relation to those reported in the literature.

Experimental Studies

Cell culture

The bacteria used in all experiments reported here were *E.*

coli AW405 (*K-12, gal-1, gal-2, thr, leu, his-4, lac, xyl, ara, strA, tonA, tsx*, and a wild type for chemotaxis) (Armstrong et al., 1967). Motile cells were selected from the outer edge of spreading colonies on swarm plates made with Luria broth and 0.2% agar (Adler, 1966). These cells were introduced to the swarm assay a second time to ensure a motile culture. Stocks were made by adding 0.15 mL of glycerol to 0.85 mL of an overnight culture, and were stored at $-55°C$. For the experiments, an inoculating loop was used to transfer a small amount of the frozen stock into 5 mL of minimal media. The inorganic portion of the minimal media consisted of 11.2-g K_2HPO_4, 4.8-g KH_2PO_4, 2.0-g $(NH_4)_2SO_4$, 0.25-g $MgSO_4 \cdot 7H_2O$, and 0.0005-g $Fe_2(SO_4)_3 \cdot 5H_2O$ per liter distilled water neutralized to pH = 7.0 (Adler and Dahl, 1967). Separately autoclaved, glucose (5 g/L) served as the carbon and energy source. Growth of this strain required the media to be supplemented with 0.25 g/L of L-threonine, L-leucine, and L-histidine. The inoculated culture, contained in a 25 ml Erlenmeyer flask, was grown in a rotary shaker (Lab-Line, Model 3527) at 150 rpm and 30°C. Cultures were harvested at an absorbance of 0.45 to 0.65 at 590 nm (Unicam SP1800 Ultraviolet Spectrophotometer). Cells were observed under phase contrast microscopy to qualitatively check for motility and contamination. The cell suspension was diluted (100-fold for population studies and 200-fold for single-cell measurements) in motility buffer (11.2-g K_2HPO_4, 4.8-g KH_2PO_4 and 0.029-g EDTA per liter distilled water) (Adler and Templeton, 1967), which had first been passed through sterile 0.2-μm filters to remove any debris or contaminant. This dilution was done directly, without intermediate washing of the cells, and resulted in an experimental cell density of approximately 2.4×10^7 cells/mL for the cell-population assay and 1.2×10^7 cells/mL for the single-cell assay. All experiments were conducted at room temperature ($25 \pm 2°C$).

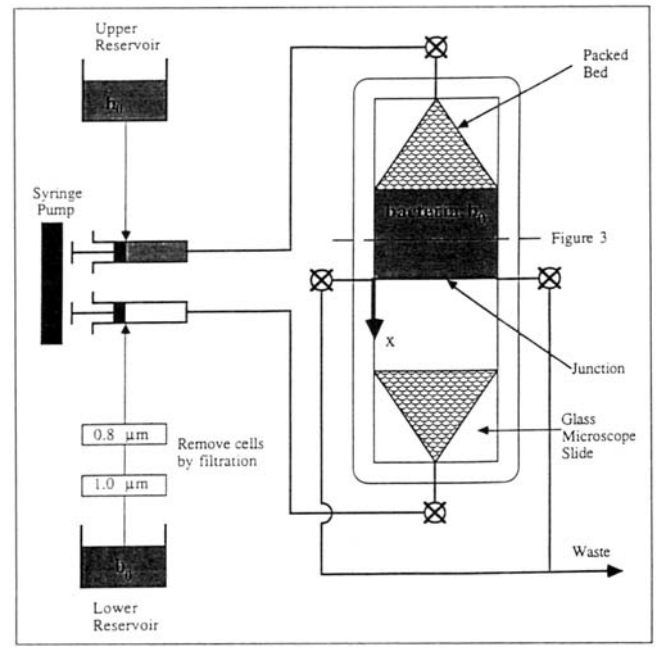

Figure 2. Stopped-flow diffusion cell (SFDC).

Fluid was fed into the upper and lower inlet ports at equal flow rates by a double-flow syringe pump. The fluid which entered the upper half of the flow cell contained bacteria at concentration b_o. Bacteria present in the reservoir leading to the lower half of the SFDC were removed by filtration before reaching the syringe pump. This prevented bacteria from entering the lower half of the flow cell. The packed bed regions (1.6-mm-dia. nylon spheres) helped disperse the flow across the width of the chamber and prevented channeling. Microscope slides used for the front and back walls of the flow cell. The SFDC was designed with a large depth to width ratio such that the fluid dynamics can be modeled as Hele-Shaw flow in two dimensions (Schlichting, 1979). The dimensions of the flow chamber, excluding the packed bed regions, are $1.5 \times 0.75 \times 0.075$ in. ($38.1 \times 19.1 \times 1.9$ mm). Dashed line indicates cross-sectional view in Figure 3.

Cell-Population Assay

Method and procedure

Random motility measurements were carried out using the stopped-flow diffusion cell (SFDC) assay. The SFDC, originally developed by Staffeld and Quinn (1989) for the study of diffusiophoresis, is similar in principle to the Mach-Zehnder interferometry cell and utilizes a flow junction method to bring in contact two fluids which differ in solute concentration (Longsworth, 1950; Caldwell et al., 1957).

The SFDC, shown in Figures 2 and 3, operates by allowing fluid to enter through the top and bottom ports and exit through the two side ports, thus establishing a flow junction. To ensure that fluid enters the upper and lower halves of the flow cell at equal flow rates, a double-syringe flow pump (Sage Instruments, Model 355) was used to feed the two inlet ports. With equal flow rates no mixing occurs between the two suspensions. It is therefore possible to establish a step gradient in solute (in this case bacteria) concentration. When flow is stopped the inlet and outlet valves are closed, producing a decaying step gradient in bacterial concentration. For a more detailed description of the SFDC, see Staffeld and Quinn (1989) and Ford et al. (1991).

Initially, all air was forced out of the SFDC and connecting tubes and replaced with motility buffer. Two reservoir flasks were used to feed the syringes which fed the inlet ports. The reservoir flask which fed the top of the SFDC contained 50 mL of the diluted cell suspension. The reservoir flask which fed the bottom of the SFDC contained 50 mL of the diluted cell suspension and 250-μL Percoll (Sigma P-1644). The Percoll was added to make the fluid in the lower half of the flow cell slightly more dense than the fluid in the upper half. This helped to stabilize the fluid within the SFDC. In-line between the bottom reservoir and the syringe pump were two membranes (Standard Nuclepore Polycarbonate Membranes) in series containing 1.0- and 0.8-μm-dia. pores, respectively. These membranes filtered off the cells before they entered the syringe and therefore prevented any cells from entering the lower half of the flow cell (see Figure 2). Placing cells in both reservoirs ensured that, with the exception of the bacteria present in the upper half of the SFDC (and Percoll in the lower half), both solutions were identical. This eliminated any potential chemical gradients to which the cells might have responded chemotactically (see Results and Discussion).

The SFDC was positioned so that a stereomicroscope (Zeiss-Model SV8) could be focused on the flow junction region. The flow cell was illuminated from behind by a fiber-optic ring light (Schott #KL 1500) emitted at a 45 deg angle producing dark-field illumination. The bacteria scatter the light, and, through a port on the microscope, a 35-mm camera (Contax

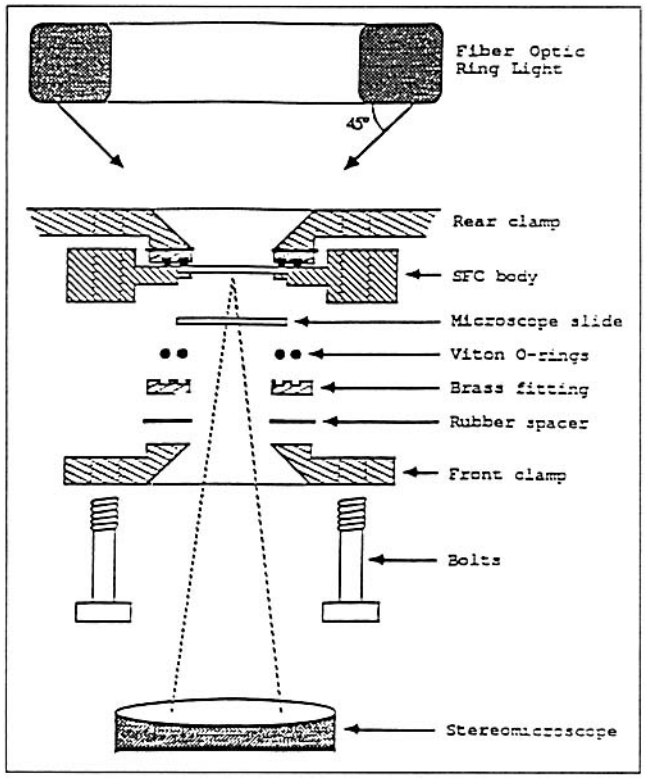

Figure 3. Partially exploded cross-sectional view of the SFDC apparatus.

Fiber-optic ring light provides dark-field illumination. Stereomicroscope had possible magnifications of 5× to 205×. Stereomicroscope adapted with a camera port parafocal with the oculars. Camera port contained a reticle which enabled pixel size to be calibrated to real dimensions during image analysis. Black and white photographs were taken with a 35-mm camera (2-s exposure) at a magnification of 12.8×.

RTS II) was used to record black and white images of the bacterial spatial distributions at discreet time points.

Data analysis

The negatives from the photographs of the bacterial spatial distributions were mounted in slide holders and the images projected via a slide projector onto a video transfer screen (Hama, model 3012). A video camera (Dage-mti, 67M Series) fitted with a 50 mm C-mount TV lens (Fujinon) was focused on the transfer screen. The image was digitized and the data were stored for analysis within an image processing system (Imaging Technology, Series 151 Image Processor). Figure 4 shows the data analysis procedure. A background image of the SFDC containing only motility buffer was subtracted from all analyzed data. The software package Mnemonics (TIPS) aided in analyzing the bacterial density profiles on each negative. Bacterial profiles were obtained by scanning the gray levels of the digitized image. The image analysis system employed allowed for 256 discreet gray levels (8 bit). The analysis was typically able to resolve 15–20 gray levels in each profile. The final profile represents the average of approximately 50 adjacent profiles (each profile one pixel in width), which in terms of the flow cell corresponds to the average concentration profile across a 3-mm front. By operating the flow cell at

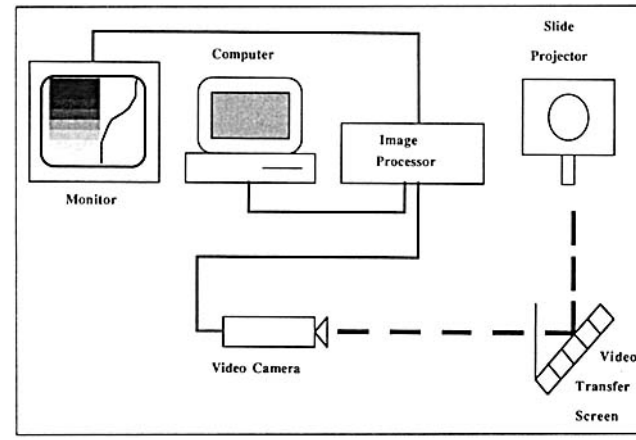

Figure 4. Cell-population data analysis procedure.

Black and white 35-mm negatives were mounted in slide holders and projected onto a video transfer screen. Video camera focused on the image. Image digitized and stored in an image processor. Bacterial profiles determined from the gray levels of the digitized images. Monitor was used to display the digitized image and concentration profile.

bacterial concentrations which scatter light linearly ($\leq 3.75 \times 10^7$ cells/mL), bacterial concentrations could be directly calibrated to gray level (Ford et al., 1991). For a more detailed description of the image analysis procedure, see Phillips (1992).

Single-Cell Assay

Method and procedure

A cell suspension (1.5×10^7 cells/mL) was placed on a glass microscope slide and covered with a cover slip supported by two other cover slips to provide sufficient volume for the cells to swim (see Figure 5). The slide was placed on a microscope stage and observed under phase contrast microscopy (Zeiss, 400×). The focal plane was established midway between the top of the microscope slide and the bottom of the cover slip in order to remove any possible wall effects. A green light

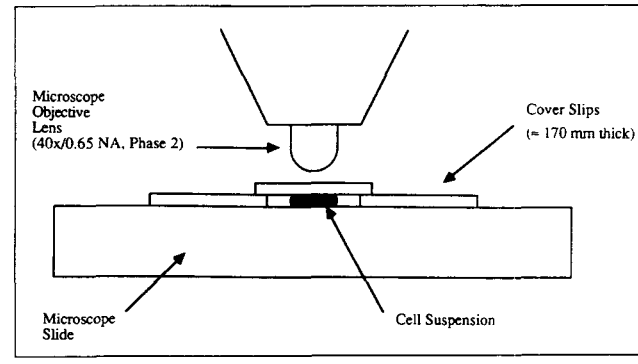

Figure 5. Single-cell assay.

Cell suspension (1.2×10^7 cells/mL) placed on a glass microscope slide. Suspension covered with cover slip supported by two other cover slips. Focal plane was established midway between the microscope slide and the cover slip. Cells video recorded in real time using phase contrast microscopy (400×). This provided a field of view (as seen on the monitor during video playback) of 283×215 μm.

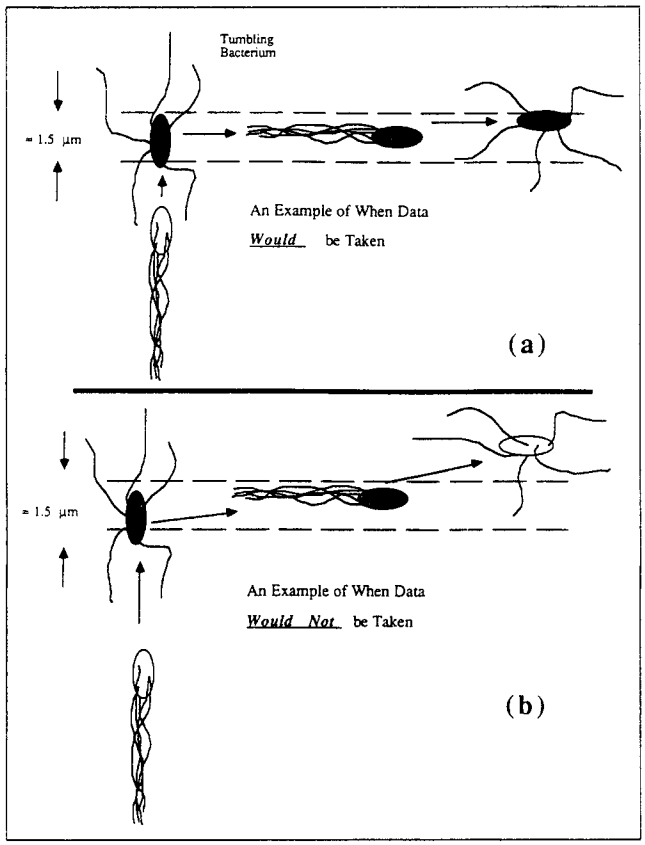

Figure 6. When single-cell motility data would and would not be recorded.

Area between the dashed lines represents the focal plane. With the microscopic and optical systems employed ($\lambda \leq 700$ nm, $NA = 0.65$), focal plane or depth of field is approximately 1.5 μm. (a) Example of when single-cell motility data *would* be taken. Cell initially outside the plane of focus and thus appears white. Cell appears dark upon entering the focal plane. Cell then tumbles, runs and tumbles again before exiting the focal plane. Data recorded representative of 3-D motility; (b) Example of when single-cell motility data *would not* be taken. Cell appears dark upon entering the focal plane and tumbles. Cell begins a run and becomes displaced outside of the plane of focus where it tumbles again. If data had been recorded, data would represent a 2-D projection of 3-D motility.

filter (Zeiss VG9) was mounted between the light source and the stage to limit the wavelength of light illuminating the cell suspension (see below). The microscope was adapted with a video camera (Dage-MTI, 67M Series) and the images recorded (JVC BR-9000U Time Lapse Video Cassette Recorder) in real time.

Data analysis

Run length time (the time between tumbles) and run displacement (the distance between tumbles) were determined directly from the video recording with the aid of image analysis technology (Imaging Technology, Series 151 Image Processor). Under phase contrast microscopy a cell within the focal plane will appear dark while a cell immediately above or below the focal plane will appear to be white. Measurements were taken only when a cell could be observed to tumble, run and then tumble again, consecutively, and when all three events took place within the focal plane (see Figure 6). The video recording was monitored until such an event was observed. The recording was then rewound to the time when the cell had just finished the first tumble and began a run. Via image analysis, the x and y pixel (512×480) position of this point was recorded. The video recording was then advanced frame by frame (30 frames/s) until the run was terminated and the second tumble began. The x and y pixel position of this point was also recorded. The run length time was obtained from the number of frames which were recorded between the two tumbles. A micrometer was used to calibrate x and y pixel displacements to real dimensions to obtain a run displacement. Finally, a run velocity was calculated by dividing the run displacement (μm) by the run length time (s).

The insertion of a green light filter between the light source and cell suspension limited the wavelength of light which illuminated the cell suspension to less than 700 nm. The focal plane can be defined as the depth of field or "setting accuracy," 2ξ, and is given by (Inoué, 1986):

$$2\xi = \frac{\lambda}{4n_i \times \sin^2\left(\frac{u}{2}\right)} \tag{1}$$

where n_i is the refractive index of the immersion medium, λ the wavelength of light and u the half angle of the cone of light that is captured by the objective lens. The numerical aperture (NA) of the objective lens and Eq. 2 can be used to calculate u:

$$u = \sin^{-1}\left(\frac{NA}{n_i}\right) \tag{2}$$

For the microscopic and optical systems employed here, Eq. 2 yields a depth of field of approximately 1.5 μm. As stated above, data were recorded only when a cell was observed to tumble, run and then tumble again, all within the focal plane. This sequence ensues when in the course of its ordinary 3-D trajectory, a bacterium executes these three steps while moving within the space defined by the focal "volume," that is, the focal plane times the depth of focus. Thus, by having a relatively thin focal "plane," the data gathered are not a two-dimensional projection of three-dimensional movement, but are instead a true representation of three-dimensional motility.

Mathematical Analysis

Cell-population assay

Due to the random walk swimming behavior of an individual bacterium, the random motility of the population can be expressed in a form analogous to that used for diffusion of inert particles (Keller and Segel, 1971):

$$\frac{\partial b}{\partial t} = \mu \frac{\partial^2 b}{\partial x^2} \tag{3}$$

where b and μ represent the bacterial density and random motility coefficient, respectively. One-spatial dimension, semi-infinite in length, is appropriate for these experimental conditions. Initially, the bacterial concentration in the upper half of the flow cell is b_o and zero elsewhere. Allowing the flow

junction in the SFDC to be represented by $x=0$ (see Figure 2), and applying these boundary and initial conditions, the solution of Eq. 3 is well known (Crank, 1975):

$$\frac{b}{b_o}=\frac{1}{2}\,\mathrm{erfc}\left(\frac{x}{\sqrt{4\mu t}}\right) \tag{4}$$

For experimental times, t, $\ll L^2/4\mu$, where L is the length of the lower half of the flow cell, the number of bacteria, $N(t)$, traveling across $x=0$ as a function of time can, from Eq. 4, be shown to be:

$$N(t)=\frac{1}{2}Ab_o\sqrt{\frac{4\mu t}{\pi}} \tag{5}$$

where A is the cross-sectional area of the flow cell. From this relationship the number of bacteria entering the lower half of the flow cell is proportional to the square root of time. By operating the flow cell at bacterial densities which scatter light linearly, the number of bacteria below the junction is proportional to the area under the concentration profile, A_p, where A_p is generated directly from image analysis of the photographic negatives. Therefore, the expression used to calculate a motility coefficient given the methods outlined above is:

$$\frac{N(t)}{A}=\frac{1}{2}b_o\sqrt{\frac{4\mu t}{\pi}}=C\cdot A_p \tag{6}$$

where the calibration constant C relates gray levels from image analysis to real bacterial densities. Again, due to the fact that these experiments are conducted with bacterial concentrations which scatter light linearly, C can be determined directly from the difference in gray level corresponding to the initial and zero bacterial densities. The gray level resulting from the initial bacterial concentration is obtained far above $x=0$ where no net flux of bacteria occurs. Similarly, the gray level corresponding to a zero concentration of bacteria can be obtained far below $x=0$ where bacteria have not yet migrated. From Eq. 6, a plot of the calibrated area vs. the square root of time should produce a linear relationship whose slope is equal to the square root of μ/π.

Single-cell assay

The theoretical models of Othmer et al. (1988) and Rivero et al. (1989) assume that the tumbling events are the result of a Poisson process with rate intensity λ_T (see Theoretical Analysis). Experimentally, the time intervals between tumbles (run length times) were measured. The derivation in the Appendix shows that if the tumbles are the result of a Poisson process, then the time intervals between tumbles are exponentially distributed with a mean equal to the inverse of the tumbling frequency or tumbling probability. Because an arithmetic mean gives no information concerning the distribution about that mean, a more accurate approach for obtaining the tumbling probability is to rearrange the data in the form of a cumulative distribution, as defined by Eq. A-6. The tumbling probability can then be obtained from the slope by plotting the natural logarithm of the fraction of run length times greater than a given time vs. time.

Theoretical Analysis

Relationship between population and single-cell parameters

The stochastic models of Othmer et al. (1988) and Rivero et al. (1989) can be used to relate the cell-population random motility coefficient to single-cell parameters as follows:

$$\mu=\frac{s^2}{n_d\lambda_T(1-\psi_d)} \tag{7}$$

where μ is the random motility coefficient, s the mean speed of the swimming cells, n_d the dimensionality of the system, λ_T the tumbling frequency or reciprocal run length time and ψ_d the index of directional persistence. The model assumes that the probability of tumbling, λ_T, is the rate intensity of a Poisson process. From probability theory (see Appendix), the mean time between tumbles is given by λ_T^{-1}. The index of directional persistence, ψ_d, accounts for the angle a cell's path takes between adjacent runs. In three dimensions, ψ_d is equivalent to the mean of the cosine of the run-to-run angle. If the angle between runs is random, the mean run-to-run angle will be 90 degrees and ψ_d will be equal to zero (see Figure 7). If the mean turn angle approaches the extreme value of 180 degrees, then on average a cell would swim in the opposite direction of its previous run and ψ_d would be equal to -1; this results in a value for the motility coefficient of one half of that which

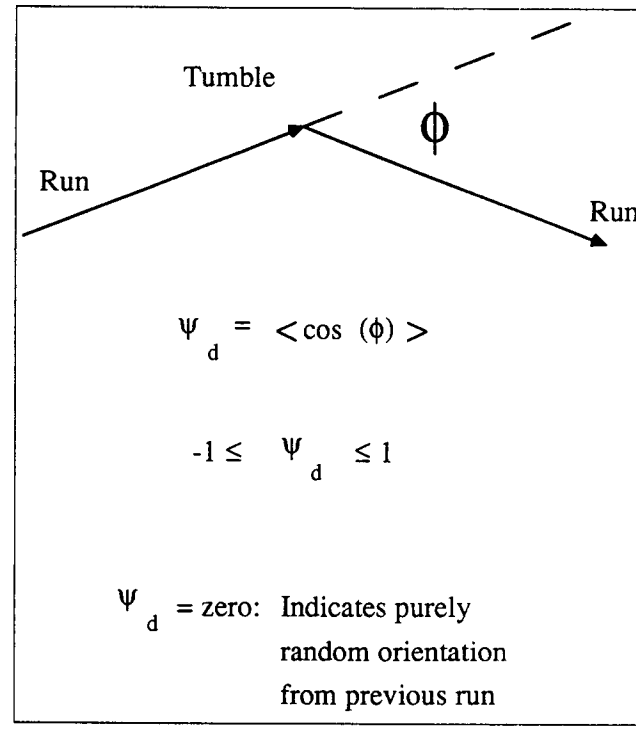

Figure 7. Run-to-run angle (ϕ) and characterization of index of directional persistence, ψ_d.

In three dimensions, index of directional persistence is defined as mean of the cosine of the run-to-run angle. If run-to-run angle was purely random, ϕ would have an expected value of 90°, resulting in a value of ψ_d equal to zero.

would be expected had the turn angle been random. A cell which only swims and never tumbles, or tumbles and then continues on in the same direction, would appear from Eq. 7 to have an infinite random motility coefficient. In this case, however, the assumption that the runs are straight (that is, noncurved) breaks down and random motility is limited by rotational Brownian motion (Berg, 1983).

Results and Discussion

Cell-population assay

Figure 8 shows the time sequence of the bacterial concentration profiles for one motility experiment. The dimensionless bacterial concentration (bacterial concentration scaled by the initial cell density, b_o) is plotted vs. position. The vertical dashed line, $x=0$, represents the flow junction of the SFDC. The baselines (horizontal dashed lines) represent the initial bacterial densities present in the flow cell. The upper baseline corresponds to the initial bacterial density, b_o, present in the upper half of the flow cell. This line was determined from the region far left of $x=0$ where the gray levels from image analysis remained constant. This corresponds to the region in the flow cell above the flow junction where there was no net flux of cells. Similarly, the lower baseline corresponds to the initial conditions in the lower half of the flow cell where there were no bacteria present and was determined from the region far right of $x=0$ where the gray levels remained constant. This corresponds to the region in the flow cell where bacteria have not yet migrated. As discussed above, when operating the flow cell at bacterial concentrations which scatter light linearly, the number of bacteria present in the lower half of the flow cell is proportional to the area of the concentration profile defined by the lower baseline, $x=0$, and the bacterial density. This will be termed the "enhanced" area. From conservation laws, the number of bacteria entering the lower half of the flow cell is equal to the number of bacteria which have left the upper half. From this and linear light scattering, the "depleted" area (defined by the upper baseline, $x=0$, and the bacterial density) is expected to be equal to the enhanced area. The average of these two areas was used in determining the random motility coefficient.

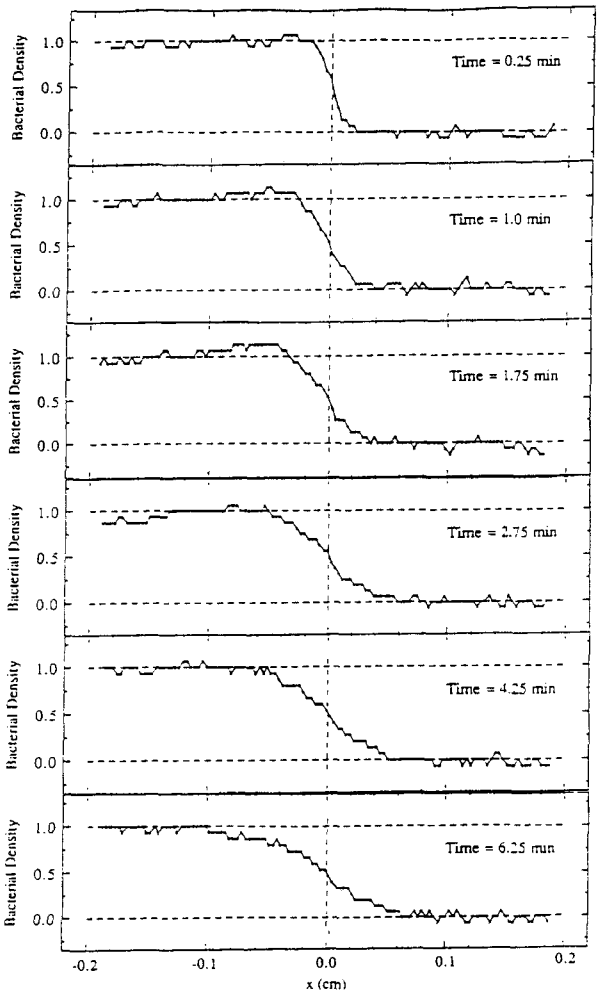

Figure 8. Time sequence of bacterial concentration profiles obtained from image analysis.

Bacterial density, scaled with the initial bacterial concentration in the upper half of the flow cell, is plotted as a function of position relative to the flow junction, $x=0$. "Enhanced" area defined by zero bacterial density, $x=0$, and bacterial concentration profile should be equal to the "depleted" area defined by the initial bacterial density, $x=0$, and bacterial concentration profile. The enhanced, depleted and average of these two areas plotted as a function of the square root of time in Figure 9.

The experimental times indicated include an "offset time" of 0.25 min to account for the "actual" initial conditions present in the SFDC when flow was stopped. The offset time is derived by comparing steady- and unsteady-state continuity equations applied to a solute (bacteria) in the flow cell under conditions of steady flow. At time equal to zero, the unsteady-state result should be the same as the steady-state result. Using this approach, the offset time, t_o, was found to be given by:

$$t_o = \frac{w}{2\pi v} \tag{8}$$

where w is the width of the chamber and v the average fluid velocity. From Eq. 8, it can be seen that an offset time can be eliminated only by operating the flow cell at an infinite flow velocity. For the experimental conditions used here, the offset time was calculated to be 0.25 min. That is, the "ideal" step function concentration profile had already decayed for 0.25 min before flow was stopped. Stated differently, a "perfect step function profile" theoretically existed 0.25 min prior to stopped flow conditions. For a rigorous analysis and further discussion of the offset time, see Staffeld and Quinn (1989).

The areas measured from concentration profiles presented in Figure 8 were plotted as a function of the square root of time and are displayed in Figure 9. The straight lines represent least-squares fits of the data. Using Eq. 6, a random motility coefficient can be obtained from the slope of this line. In the example shown here, the random motility coefficient was found to be 2.1×10^{-6} cm^2/s. It is important to note that the intercept of this line is equal to zero. This indicates that no cells have crossed from the upper to the lower half of the flow cell at time equal to zero, an ideal step function in bacterial concentration. This would not have been the case had not the offset time been included in this analysis. Instead, the y-intercept would have been equal to the area expected for a step function already having decayed for a time period equal to the offset time. In four experiments, the random motility coefficient was determined to be $1.9\ (\pm0.3)\times10^{-6}$ cm^2/s.

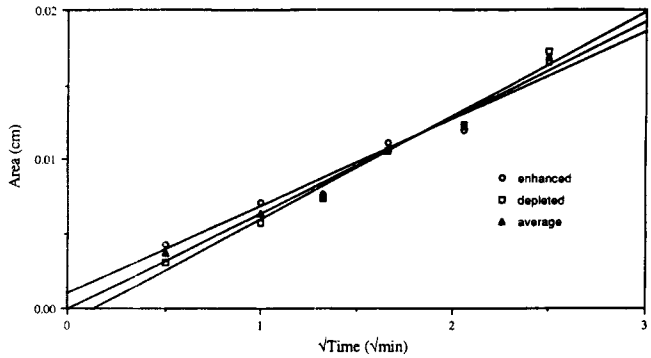

Figure 9. Enhanced (○), depleted (□) and average of these two areas (△) displayed in Figure 8 as a function of the square root of time.

Random motility coefficient can be obtained from the slope. In this example, using the average area, a random motility coefficient of 2.1×10^{-6} cm^2/s was determined.

Due to its experimental simplicity, the capillary assay is the most commonly used technique in measuring bacterial motility (Adler, 1973). For random motility measurements, a capillary tube, approximately 1 μL in volume, is sealed at one end and filled with motility buffer. The tip of the open end is then placed into a chamber containing a known bacterial concentration suspended in motility buffer. As time passes, bacteria will begin to accumulate in the tube. After a given time interval, usually one hour, the number of bacteria in the tube, $N_c(t)$, are counted and a random motility coefficient is determined from Eq. 9 (Segel et al., 1977):

$$\mu=\frac{\pi}{4t}\left(\frac{N_c(t)}{\pi R^2 C_o}\right)^2 \tag{9}$$

where t is time, R the inner radius of the capillary tube and C_o the initial bacterial density in the chamber. Equation 9 is obtained from the same formalism used in deriving Eq. 5 with the assumption that the bacterial concentration at the open end of the tube is constant and equal to C_o.

The first measurements of a random motility coefficient were reported by Adler and Dahl (1967). Using a slight variation of the capillary assay, they measured the random motility coefficient of *E. coli* B275 to be approximately 7.0×10^{-5} cm^2/s. Using data presented by Adler (1969) obtained from the capillary assay while investigating the motility of *E. coli* W3110, Segel et al. (1977) calculated a random motility coefficient of 8.3×10^{-6} cm^2/s. In the same investigation and conducting their own capillary experiments, they measured the motility coefficient of *Pseudomonas fluorescens* to be 5.6×10^{-6} cm^2/s. Rivero-Hudec and Lauffenburger (1986), using capillary assay data presented by Adler (1973), calculated the random motility coefficient of *E. coli* B14 to be 5.4×10^{-5} cm^2/s. From capillary assay data presented by Mesibov et al. (1973) and Eq. 9, we were able to determine the random motility coefficient for *E. coli* AW518 and *E. coli* 20SOK$^-$. From 13 experiments conducted on five different cultures, values for the random motility coefficient of AW518 ranged from 7.5×10^{-6} to 3.5×10^{-5} cm^2/s, with a mean and standard deviation of 1.4×10^{-5} and 0.5×10^{-5} cm^2/s, respectively. For 20 experiments conducted on the same culture, values for the random motility coefficient of 20SOK$^-$ ranged from 4.9×10^{-5} to 3.7×10^{-4} cm^2/s, with a mean and standard deviation of 1.9×10^{-4} and 0.9×10^{-4} cm^2/s, respectively.

Using a light scattering densitometer, Holz and Chen (1979) concluded that the random motility coefficient of *E. coli* K12 lies in the range $1\text{-}10\times10^{-7}$ cm^2/s. Dahlquist et al. (1972) used a light scattering apparatus to investigate the motility of *Salmonella typhimurium*. From the data, Segel and Jackson (1973) calculated the random motility coefficient to be 6×10^{-5} cm^2/s. In this laboratory, using the stopped-flow diffusion cell, Ford et al. (1991) measured the random motility coefficient of *E. coli* NR50 to be $1.1\ (\pm0.4)\times10^{-5}$ cm^2/s. Berg and Turner (1990), using a fused array of 50 μm diameter capillary tubes, measured the random motility coefficient of *E. coli* AW405 to be $2.6\ (\pm0.4)\times10^{-6}$ cm^2/s. A summary of these results is presented in Table 1.

Our value for the random motility coefficient of *E. coli* AW405 compares well with that of Berg and Turner (1990). Discrepancies between the two values may possibly be attributed to differences in cell culturing and experimental condi-

Table 1. Measured Values of the Random Motility Coefficient

Species	μ (cm^2/s)	Reference
Pseudomonas Fluorescens	$6\ (\pm2)\times10^{-5}$	Segel et al. (1977)***
Salmonella typhimurium	6×10^{-5}	Dahlquist et al. (1972)*
		Segel and Jackson (1973)**
Escherichia coli K12	$1\text{-}10\times10^{-7}$	Holz and Chen (1979)***
Escherichia coli 20SOK	$1.9\ (\pm0.9)\times10^{-4}$	Mesibov et al. (1973)*†
Escherichia coli AW518	$1.4\ (\pm0.5)\times10^{-5}$	Mesibov et al. (1973)*†
Escherichia coli B14	5.4×10^{-5}	Adler (1973)*
		Rivero-Hudec and Lauffenburger (1986)**
Escherichia coli NR50	$1.1\ (\pm0.4)\times10^{-5}$	Ford et al. (1991)**
Escherichia coli W3110	8.3×10^{-6}	Adler (1969)*
		Segel et al. (1977)**
Escherichia coli B275	6.9×10^{-5}	Adler and Dahl (1967)***
Escherichia coli B275	7.2×10^{-5}	Adler and Dahl (1967)***
Escherichia coli AW405	$2.6\ (\pm0.4)\times10^{-6}$	Berg and Turner (1990)***
Escherichia coli AW405	$1.9\ (\pm0.3)\times10^{-6}$	This investigation

*Source of experimental data.
**Source where the random motility coefficient was calculated based on the experimental data.
†Random motility coefficient calculated from Eq. 9.

tions. The cells in this investigation were grown on glucose in a minimal salts medium whereas theirs were grown on a richer tryptone broth medium. Lowe et al. (1987) found that for *E. coli* HCB437, the rotational frequency of the coordinated flagellar bundle was much higher for cells grown on tryptone broth than for cells grown on glycerol in a minimal salts medium. This translates to a higher swimming speed for cells grown in the richer medium. Also, the experiments in this investigation were performed at room temperature ($25 \pm 2°C$) whereas those of Berg and Turner were conducted at 30°C. A linear dependence of swimming speed on temperature has been observed for both *E. coli* and *Salmonella typhimurium* (Lowe et al., 1987; Banks et al., 1975; Maeda et al., 1976; Miller and Koshland, 1977).

As stated above, Berg and Turner (1990) measured their random motility coefficient for cells swimming in capillary tubes of diameter 50 μm. In their investigation, they also found that the value of the random motility coefficient increased by a factor of 2.3 when measurements were made using 10-μm capillaries. It appears that in the smaller capillary tubes motility occurs predominantly along the axial direction; this observation is consistent with realistic simulations of motility in small capillaries (Phillips and Quinn). Although the motility values obtained with the 10 and 50 μm capillaries are different, it is not evident that the 50 μm capillary is equivalent to that of a bulk phase. The macroscopic dimensions of the SFDC provide unhindered, bulk phase and three-dimensional motility.

It is difficult to make other comparisons of the data presented in Table 1 since these measurements have been carried out on a variety of species and strains. The culturing and experimental conditions in many cases vary from laboratory to laboratory, and, as discussed above, these factors also effect motility. In general, it appears that the random motility coefficient may vary over two orders of magnitude among different species and strains. If these bacteria were immotile, they would still "diffuse" as a result of Brownian motion. Using Stokes law, this yields a motility or diffusion coefficient of approximately 2×10^{-9} cm^2/s (Berg, 1983).

The random motility coefficient was also measured at two different uniform concentrations of serine, an amino acid known to effect the motility of this strain (Berg and Brown, 1972). Conducting four experiments at a serine concentration of 6.7×10^{-5} molar, the random motility coefficient was found to be $3.8\ (\pm 0.4) \times 10^{-6}$ cm^2/s. At 1×10^{-3} molar serine, a random motility coefficient of $8.9\ (\pm 0.5) \times 10^{-6}$ cm^2/s was measured. These data are presented in Table 2. Holz and Chen (1979) used their light-scattering densitometer and determined the random motility coefficient of *E. coli* K12 as a function of serine concentration. At a concentration of 1×10^{-3} molar serine they observed approximately a 2-fold increase in their calculated value of the random motility coefficient. At this same serine concentration and from the data presented in Table 2, a 4.7-fold increase was observed in this investigation. In the absence of serine the measured value of the random motility coefficient determined here was more than twice their reported value.

Table 2. Measured Values of the Random Motility Coefficient as a Function of Serine Concentration*

L-Serine Concentration (10^{-5} Molar)	μ (10^{-6} cm^2/s)
0	1.9 ± 0.3
6.7	3.8 ± 0.4
100	8.9 ± 0.5

*Date presented as mean ± one standard deviation.

As stated above, it was necessary to place bacteria in the reservoirs leading to both the upper and lower halves of the flow cell. The cells in the reservoir leading to the lower half of the SFDC were then removed by filtration. This was to ensure that except for the presence of cells in the upper half of the flow cell (and Percoll in the lower half), both solutions were identical. When cells were not placed in the lower reservoir, a thin band of migrating cells was seen to form just below the flow junction. In some instances this band was observed to form immediately after flow was stopped, and at other times it became visible over time. The formation of this band is indicative of a chemotactic response. It is well known that both *E. coli* and *Salmonella typhimurium* respond chemotactically towards oxygen (Baracchini and Sherris, 1959; Adler, 1966; Laszlo and Taylor, 1981; Shioi et al., 1987). We believe that due to the endogenous metabolism of the cells, the oxygen concentration in the upper reservoir was reduced while the oxygen concentration in the lower reservoir, containing only motility buffer, remained saturated. Upon introducing these two fluids into the flow cell, a gradient in oxygen concentration formed at the flow junction. Cells swimming near the flow junction region chemotactically responded to the oxygen gradient. The band was, at most times, easily detectable by the naked eye. Band formation was observed when the reservoir containing cells was fed to either the upper or lower half of the flow cell. Band formation also occurred when Percoll was absent from the lower reservoir (cells were not responding chemotactically to Percoll). In all cases, the band did not move far from the junction. In some experiments, a second, and possibly a third band could be seen to form above the first band. Band formation did not occur when cells were placed in the reservoir leading to the lower half of the flow cell and then removed by filtration.

Single-Cell Assay

Cell velocity

The velocity distribution for bacteria swimming in the absence of serine is presented in Figure 10. The data were distributed normally or slightly skewed from normal with a mean (± standard deviation) of 24.1 ± 6.8 μm/s. A total of 260 velocity measurements were gathered from three different cell cultures. The measurements from each culture gave approximately the same distribution. Since the data were gathered only when a bacterium was observed to tumble, run, and then tumble again, and when all three events occurred within the focal plane, it was rare that motility parameters for a single bacterium were measured more than once. In the rare instance when an individual bacterium was observed to complete two consecutive runs within the focal plane the velocity was found to be relatively constant.

The following is a discussion of previously measured values of cell velocity which have been reported in the literature. Using cinematography techniques, Maeda et al. (1976) measured the swimming speed of *E. coli* W3110 to be approximately 28 μm/s at 25°C, approximately the same experimental temper-

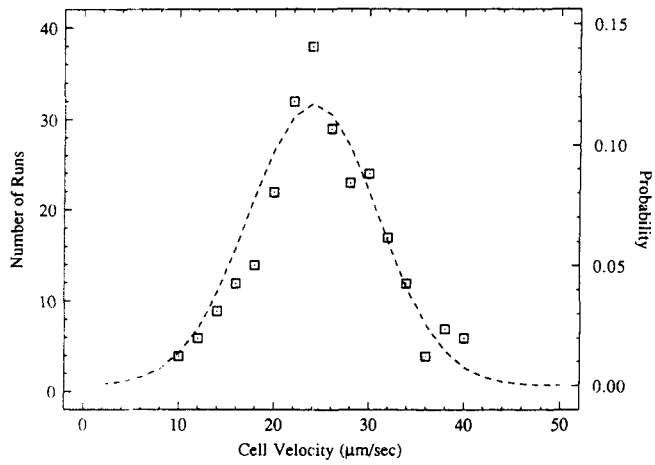

Figure 10. Distribution of cell velocities.

Cell velocities were grouped in 2 μm/s-wide bins. The number of runs of a given cell velocity displayed on lefthand side. The righthand side shows the fraction of runs of a given cell velocity expressed as probability. A total of 260 measurements were taken from three different cell cultures. (Not shown is one cell velocity measured to be 61.3 μm/s.) The mean (±standard deviation) was found to be 24.1 ± 6.8 μm/s. Dashed line represents a normal distribution based on this mean and standard deviation.

ature used in this investigation. They also determined that the swimming velocity increased with increasing temperature. Using number fluctuation spectroscopy, Banks et al. (1975) measured the swimming speed of a smooth swimming strain of *E. coli* at 25°C to be 16 μm per second. They also found a linear relationship between cell speed and temperature between 25 and 35°C. Nossal and Chen (1973) used the technique of laser intensity correlation spectroscopy and determined the root mean square speed of a wild type *E. coli* K12. At 25 ± 2°C, they measured a value of approximately 10–15 μm/s. Using stroboscopic photography, Macnab and Koshland (1972) measured the velocity of *Salmonella typhimurium* to be 28.8 ± 5.1 μm/s. Schneider and Doetsch (1974) measured cell velocity directly from videotape. Conducting experiments at 21°C on two different cultures of *Serratia marcescens*, they determined the velocity to be approximately 43.4 μm/s. They found no statistical difference of velocity measurements between the two cultures. Taylor and Koshland (1975) also made measurements directly from videotape while investigating motility responses to light. They determined the swimming velocity of *Salmonella typhimurium* to be 34.6 μm/s. Poole et al. (1988) used real-time computer tracking to measure the velocity of *Salmonella typhimurium*. From 211 cell tracks they determined a velocity of 18.4 ± 8.8 μm/s. The distribution of these velocities appear to be normal to skewed-normal.

The most thorough investigation of single-cell bacterial motility was carried out by Berg and Brown (1972) using a three-dimensional tracking microscope (Berg, 1971). The tracking microscope automatically follows individual cells as they swim in three dimensions and digitally records their position at a rate of 12.6 data points per second. Their experiments were conducted at 32°C in a motility medium with 0.18 percent (w/v) hydroxypropyl methylcellulose which increased the viscosity of the medium to 2.7 cp. It has been shown that cell velocity is nearly optimum under these viscous conditions (Schneider and Doetsch, 1974; Greenberg and Canale-Parola, 1977). The tracking microscope provided for a detailed analysis of swimming velocity, run length time, tumbling time, and turn angle (index of directional persistence). Using *E. coli* AW405, they measured these parameters for a total of 35 bacteria from three different cell cultures. Mean swimming speed was found to be 14.2 ± 3.4 μm/s and not strongly skewed. They also found that speed is nearly uniform during a run. Our value of the velocity determined for the same strain was significantly higher at 24.1 ± 6.8 μm/s. It is not clear whether or not this difference can be attributed to experimental methods. In both investigations cells were grown in a minimal salts medium, the only difference being that they used glycerol as the carbon source whereas we used glucose. Their experiments were conducted at a higher temperature than those reported here. Lowe et al. (1987) used the tracking microscope and determined a linear relationship between swimming speed and temperature. At 32°C, they determined the velocity of *E. coli* AW405 grown in a rich T broth medium to be 36.4 ± 1.0 μm/s.

Cell velocity measurements were also determined at the same two uniform concentrations of serine at which the population studies were conducted. At a uniform concentration of 6.7×10^{-5} and 1×10^{-3} molar serine, cell speed was found to be 30.7 ± 7.1 and 30.2 ± 5.2 μm/s, respectively (see Table 3). This corresponds to approximately a 25 percent increase compared to cell speeds measured in the absence of serine. These distributions also appeared to be slightly skewed of normal. Macnab and Koshland (1972) found that the velocity of *Salmonella typhimurium*, a related species, remained essentially unchanged at serine concentrations up to 1×10^{-3} molar. Nossal and Chen (1973) determined the root mean square velocity of *E. coli* K12 over a range of serine concentrations. Cell speed was found to increase with increasing concentrations of serine up to 1×10^{-2} molar where it peaked. At this concentration, cell speed was over 30 μm/s, more than double that in the absence of serine. Berg and Brown, using the same strain, also studied the effect of serine on motility and found that cell speed increased 40 percent as serine concentration was increased to 1×10^{-3} molar.

In brief, the value of cell speed determined in this investigation is consistent with those reported in the literature. The fact that the value presented here is higher than that reported by Berg and Brown for the same bacterial strain may be due to differences in experimental conditions. In addition, the trend

Table 3. Measured Values of Single-Cell Motility Parameters as a Function of Serine Concentration*

L-Serine Concentration (10^{-5} Molar)	Cell Speed (μm/s)	Mean Run Length Time** (s)	Tumbling Probability† (1/s)
0	24.1 ± 6.8	0.84 ± 0.71	1.37
6.7	30.7 ± 7.1	1.00 ± 0.87	1.15
100	30.2 ± 5.2	1.35 ± 1.02	0.67

*Data presented as mean ± one standard deviation. With no serine present, a total of 260 velocity and run length measurements were gathered. A total of 280 and 308 measurements were obtained for the intermediate and high serine concentrations, respectively. Each data set was gathered from three different cell cultures.

**For ideal exponential distribution the mean is equal to the standard deviation.

†Obtained from Eq. A6. For ideal Poisson statistics should be equal to the inverse of the mean run length time in column 3.

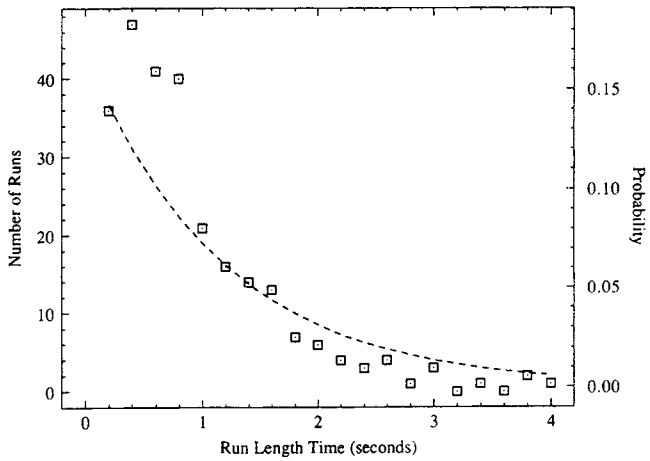

Figure 11. Distribution of cell run length times.

Cell run length times were grouped in 0.2 s-wide bins. The number of runs of a given time length are displayed on the left-hand side. Righthand side shows the fraction of runs of a given time length expressed as a probability. A total of 260 measurements were taken from three different cell cultures. The mean and standard deviation were found to be 0.84 and 0.71 s, respectively. For an ideal exponential distribution the mean and standard deviation have the same value. Dashed line represents an exponential distribution based on the mean and is given by Eq. A5.

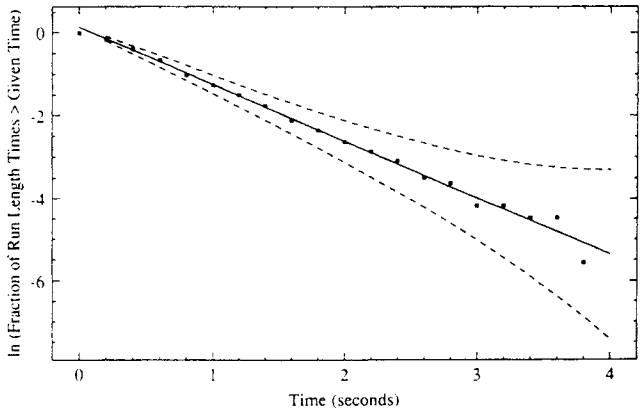

Figure 12. Distribution of the cell run length times presented in Figure 11, as defined by Eq. A6.

Natural logarithm of the fraction of run length times greater than a given time are plotted as a function of time (solid squares). Solid line represents the least-squares fit of the data. From Eq. A6 the tumbling probability is obtained from the slope. In this case, the tumbling probability was found to be 1.37/s. This corresponds to a mean run length time of 0.73 s. Dashed lines represent the theoretical standard deviation from the least-squares fit and are obtained from Eq. A7.

of serine enhanced velocity reported by other investigators was also observed here.

Cell run length time

The distribution of run length times for bacteria swimming in the absence of serine is shown in Figure 11. The data were distributed exponentially with a mean (●standard deviation) of 0.84 ± 0.71 s. As noted in the Appendix, the standard deviation of an exponential distribution has the same value as the mean. In Figure 12, the same data are plotted as defined by Eq. A6. The tumbling probability can be obtained from the slope. In this case the tumbling probability was found to be 1.37 per second. This corresponds to a mean run length time of 0.73 s, comparable to the value determined from the arithmetic mean of the data presented in Figure 11. The y-intercept of a true exponential distribution logarithmically plotted in accordance with Eq. A6 would be expected to be equal to zero. That is, all run length times are greater than zero. In Figure 12, the intercept was found to be 0.13. This is due to the fact that the exponential distribution displayed in Figure 11 appears to be incomplete at short run length times. The reason for this can be partially attributed to an uncertainty in the experimental technique when measuring short run length times. When a run appeared to occur over only a few frames, it was sometimes very difficult to locate exactly when the first tumble ended and the run began and also when the run ended and the second tumble began. For this reason, many of these runs were not recorded. Thus, the distribution at very short run length times is somewhat incomplete. This could be accounted for by rewriting Eq. A6:

$$\ln (g) = \lambda_T (t - t^*) \tag{10}$$

where t^* is the shortest measurable run length time. An approximation of t^* can be obtained from the intercept and slope of a least-squares fit line. Setting $y = 0$, t^* is approximated to be 0.095 s. At 30 frames per s, this corresponds to runs of length less than or equal to three frames. As described above, it was the run times of this length and less which were very often not measured due to the uncertainty of the run-tumble distinction. This variation of the analysis, however, did not effect the tumbling probability.

Maeda et al. (1976) measured the tumbling frequency as a function of temperature for *E. coli* W3110. The tumbling frequency was found to have a sharp peak at 34°C and was very low at both 39 and 20°C. At 25°C the tumbling frequency was approximately 0.3 per s corresponding to a mean run length time of 3.33 s. Lowe et al. (1987) used the tracking microscope and measured the mean run length time of *Streptococcus* strain V4051 to be 1.71 ± 0.90 s. They also found the run statistics to be Poisson. Berg and Brown (1972) used the tracking microscope and measured the mean (±standard deviation) run length time of *E. coli* AW405 to be 0.86 ± 1.18 s. This compares well with the value measured in this investigation of 0.84 ±0.71 s.

Run length times were also measured at two uniform concentrations of serine. At a concentration of 6.7×10^{-5} molar serine, the run length time distribution was exponential with a mean (±standard deviation) of 1.00 ± 0.87 s. From Eq. A6 the tumbling probability was determined to be 1.15 per s. At a serine concentration of 1×10^{-3} molar, the run length time distribution was again exponential with a mean (±standard deviation) of 1.35 ± 1.02 s. From Eq. A6 the tumbling probability was determined to be 0.67 per s. These data are presented in Table 3. We believe that at this high serine concentration the value for the mean run length time may be underestimated (tumbling probability overestimated). This is due to the limited field of view as displayed on the video monitor (see Single-Cell Assay *Method and Procedure*). The field of view on the monitor is 283×215 μm (349 μm diagonally). A cell swimming

at 30 μm/s along the short axis will traverse the field of view in 7.2 s. A cell which began its run in the exact middle of the field of view could at most remain in the field for 5.8 s at this same velocity. At the high serine concentration, cells were frequently observed to swim from 4 to 7 s, becoming displaced outside of the field of view before completing the run (tumbling). Thus, the limited field of view may bias run length time distributions away from longer runs. The field of view can be increased by lowering the magnification, however, visualization of the cells then becomes difficult. The depth of the field (Figure 6) also biases run length times away from longer runs. A cell swimming within the focal plane, not exactly parallel to the field of view will, over time, become displaced above or below the plane of focus. The longer the run displacement the more likely that this will occur. Furthermore, small influences due to rotational diffusion would amplify this effect. It is obvious that the limited field of view and narrow focal plane would also affect measurements taken on cells swimming in the absence of or at the intermediate concentration of serine. Due to shorter run length times, and, in the case of no serine, a slower velocity, these influences would not be as crucial a factor in these cases. However, the general effect of the limited field of view and the narrow focal plane biases run length time distributions away from longer runs. This results in possibly underestimating both the mean and standard deviation of the distributions.

Berg and Brown have also measured the effect of serine on the run length times for *E. coli* AW405 and found that as the serine concentration is increased the distributions remain exponential but are shifted towards longer runs. At a concentration of 6.7×10^{-5} molar serine, they found the mean run length time to increase approximately 2.5-fold over that observed in the absence of serine. This corresponds to a mean run length time of 2.15 s. At 1×10^{-3} molar serine, the mean run length time increased 3.5-fold corresponding to a mean run length time of 3.0 s. Although we also observed an increasing mean run length time as a function of serine concentration, the effect was not as pronounced.

We found no correlation between cell velocity and run length time. Linear correlation coefficients both in the absence and presence of serine were less than 0.1. Brown (1974) found cell speed to be correlated with run length time. From 73 measurements on an individual bacterium, he determined a linear correlation coefficient of 0.72.

Theoretical comparison of cell-population and single-cell parameters

Due to the relative infrequency of the event in which an individual bacterium remains in the focal plane for two consecutive runs, the index of directional persistence, ψ_d, could not be measured directly. However, Eq. 7 and the data presented in Tables 2 and 3 can be used to estimate the index of directional persistence. In the absence of serine and using the tumbling probability obtained from Figure 12, ψ_d was determined to be 0.26. This indicates a positive directional persistence in the random motility behavior. Berg and Brown, using the tracking microscope, directly measured the run-to-run angle and calculated ψ_d to be 0.3 (Brown, 1974). Lowe et al. (1987), also using the tracking microscope, measured the run-to-run angle of a *Streptococcus* strain and determined approximately the same value for ψ_d.

At the intermediate and high serine concentrations, ψ_d was determined to be 0.28 and 0.49, respectively. Berg and Brown determined that the mean change in direction from run-to-run decreased 40% at higher serine concentrations resulting in a slightly higher value of ψ_d. This is the same trend observed in this investigation. We believe, however, that our value of 0.49 at the high serine concentration may be overestimated due to an overestimated tumbling probability as discussed above. Brown (1974) found no correlation between change in direction and cell speed or run length time.

Conclusions

This is the first investigation in which random motility parameters have been measured at both the cell-population and single-cell levels. The SFDC has proven to be a reliable and precise method for measuring the random motility coefficient of a cell population. It has produced highly reproducible results which are consistent with the few published results to which direct comparison can be made. Random motility coefficients were also measured in the presence of two different uniform concentrations of serine; values were observed to increase with increasing concentrations of serine, as expected.

We have also developed a very simple optical technique to measure the single-cell motility parameters, speed and run length time. The distribution of cell velocities was found to be slightly skewed of normal. Run length time distributions were determined to be exponential. From the run length time distribution a tumbling probability was calculated. The values and distributions of these single-cell parameters are consistent with those reported in the literature. Single-cell parameters were also measured at the same two uniform concentrations of serine used in the population studies. The mean speed value was found to increase slightly in the presence of serine. As the concentration of serine increases, the run length time distribution remains exponential but is shifted towards longer times. These trends are also consistent with reports in the literature. The limitation of this technique is that it does not readily permit for measurement of the turn angle between two consecutive runs. The event in which a cell makes two consecutive runs while remaining in the focal plane is relatively rare.

The theoretical expressions of Othmer (1988) and Rivero et al. (1989) were used to estimate the index of directional persistence from the random motility coefficient measured using the SFDC, and the cell speed and tumbling probability determined microscopically. The values obtained also appear to be consistent with the limited values reported in the literature. From this comparison it appears that the theoretical expression relating the cell-population random motility coefficient to single-cell parameters is valid for a bacterium swimming in three-dimensions. The agreement of these two experimental methods demonstrates that the macroscopic transport behavior of a population of motile bacteria can be predicted from microscopic observations on single cells.

The single-cell observation technique presented here is a simple and straightforward method for obtaining detailed motility measurements. This approach, however, does not readily permit for measurement of the index of directional persistence. This limitation is due to the relative rarity of a cell executing two consecutive runs while remaining in the focal plane. With advanced image analysis however, this technique could be au-

tomated, thereby overcoming this limitation. This method would then provide a means for complete and detailed characterization of bacterial random motility.

Acknowledgment

The authors would like to thank Dr. Paul DiMilla for valuable discussions concerning the interpretation of results presented here. This investigation was supported in part by National Science Foundation Grant BCS86-12987.

Notation

a = time
A = cross-sectional area of flow cell
A_p = area defined by the bacterial concentration profile
b = bacterial density
b_o = initial bacterial density
C = calibration constant relating bacterial density to gray level
C_o = initial bacterial density in the capillary assay chamber
g = fraction of run length times greater than some time t
L = length of the lower half of the flow cell
n = number of tumbles
n_d = dimensionality of system
n_i = refractive index
N = number of bacteria moving from the upper to the lower half of the flow cell
N_c = number of bacteria accumulated in the capillary tube
N_P = total number of tumbles
N_R = total number of runs
NA = numerical aperture of objective lens
P = probability
R = inner radius of capillary tube
s = cell speed
t = time
t_o = offset time
t^* = shortest run length time which can be measured
T_n = time between the $(n-1)$st tumble and the nth tumble
u = half angle of the cone of light gathered by the objective lens
v = average fluid velocity inside the flow cell
w = flow cell width
x = position in flow cell relative to flow junction

Greek letters

λ_T = tumbling probability
λ = wavelength of light
μ = random motility coefficient
ξ = one half of the focal plane thickness
σ = standard deviation
ψ_d = index of directional persistence

Literature Cited

Adler, J., "Chemotaxis in Bacteria," *Sci.*, **153**, 708 (1966).
Adler, J., "Chemoreceptors in Bacteria," *Sci.*, **166**, 1588 (1969).
Adler, J., "A Method for Measuring Chemotaxis and Use of the Method to Determine Optimum Conditions for Chemotaxis by *Escherichia coli*," *J. Gen. Microbiol.*, **74**, 77 (1973).
Adler, J., and M. M. Dahl, "A Method for Measuring the Motility of Bacteria and for Comparing Random and Non-random Motility," *J. Gen. Microbiol.*, **46**, 161 (1967).
Adler, J., and B. Templeton, "The Effect of Environmental Conditions on the Motility of *Escherichia coli*," *J. Gen. Microbiol.*, **46**, 175 (1967).
Alweiss, B., J. Dostal, K. E. Carey, T. F. Edwards, and R. Freter, "The Role of Chemotaxis in the Ecology of Bacterial Pathogens of Mucosal Surfaces," *Nature*, London, **266**, 448 (1977).
Armitage, J. P., A. Gallagher, and A. W. B. Johnston, "Comparison of the Chemotactic Behavior of *Rhizobium leguminosarum* with and without the Nodulation Plasmid," *Molecular Microbiol.*, **2**, 743 (1988).
Armstrong, J. B., J. Adler, and M. M. Dahl, "Nonchemotactic Mutants of *Escherichia coli*," *J. Bacteriol.*, **93**, 390 (1967).
Banks, G., D. W. Schaefer, and S. S. Alpert, "Light-scattering Study of the Temperature Dependence of *Escherichia coli* Motility," *Biophys. J.*, **15**, 253 (1975).
Baracchini, O., and J. C. Sherris, "The Chemotactic Effect of Oxygen on Bacteria," *J. Pathol. Bacteriol.*, **77**, 565 (1959).
Berg, H. C., "How to Track Bacteria," *Rev. Sci. Instrum.*, **42**, 868 (1971).
Berg, H. C., *Random Walks in Biology*, Princeton University Press, Princeton, NJ (1983).
Berg, H. C., and R. A. Anderson, "Bacteria Swim by Rotating their Flagellar Filaments," *Nature*, London, **245**, 380 (1973).
Berg, H. C., and D. A. Brown, "Chemotaxis in *Escherichia coli* Analysed by Three-dimensional Tracking," *Nature*, London, **239**, 500 (1972).
Berg, H. C., and L. Turner, "Chemotaxis of Bacteria in Glass Capillary Arrays," *Biophys. J.*, **58**, 919 (1990).
Blanc-Lapierre, A., and R. Fortet, *Theory of Random Functions*, Vol. 1, Gordon and Breach Science Publishers, New York (1965).
Brown, D. A., "Chemotaxis in *Escherichia coli*," PhD Thesis, University of Colorado, Boulder (1974).
Brown, D. A., and H. C. Berg, "Temporal Stimulation of Chemotaxis in *Escherichia coli*," *Proc. Nat. Acad. Sci. USA*, **71**, 1388 (1974).
Caldwell, C. S., J. R. Hall, and A. L. Babb, "Mach-Zehnder Interferometer for Diffusion Measurements in Volatile Liquid Systems," *Rev. Sci. Inst.*, **28**, 816 (1957).
Chet, I., P. Asketh, and R. Mitchell, "Repulsion of Bacteria from Marine Surfaces," *Appl. Microbiol.*, **30**, 1043 (1975).
Crank, J., *The Mathematics of Diffusion*, 2nd ed., Clarendon, Oxford (1975).
Dahlquist, F. W., P. Lovely, and D. E. Koshland, Jr., "Quantitative Analysis of Bacterial Migration in Chemotaxis," *Nature New Biology*, London **236**, 120 (1972).
Farrell, B. E., R. P. Daniele, and D. A. Lauffenburger, "Quantitative Relationships Between Single-Cell and Cell-Population Model Parameters for Chemosensory Migration," *Cell Motility and the Cytoskeleton*, **16**, 279 (1990).
Ford, R. M., B. R. Phillips, J. A. Quinn, and D. A. Lauffenburger, "Measurement of Bacterial Random Motility and Chemotaxis Coefficients: I. Stopped-Flow Diffusion Chamber Assay," *Biotech. Bioeng.*, **37**, 647 (1991).
Freter, R., P. C. M. O'Brien, and M. S. Macsai, "Role of Chemotaxis in the Association of Motile Bacteria with Intestinal Mucosa: In Vivo Studies," *Infec. Immun.*, **34**, 234 (1981).
Gannon, J. T., V. B. Manilal, and M. Alexander, "Relationship Between Cell Surface Properties and Transport of Bacteria through Soil," *Appl. Environ. Microbiol.*, **57**, 190 (1991).
Greenberg, E. P., and E. Canale-Parola, "Motility of Flagellated Bacteria in Viscous Environments," *J. Bact.*, **132**, 356 (1977).
Gulash, M., P. Ames, R. C. Larosiliere, and K. Bergman, "Rhizobia are Attracted to Localized Sites on Legime Roots," *Appl. Env. Microbiol.*, **48**, 149 (1984).
Hall, R. L., "Amoeboid Movement as a Correlated Walk," *J. Math. Biol.*, **4**, 327 (1977).
Holz, M., and S. H. Chen, "Spatio-temporal Structure of Migrating Chemotactic Band of *Escherichia coli* I. Travelling Band Profile," *Biophys. J.*, **26**, 243 (1979).
Inoué, S., *Video Microscopy*, Plenum Press, New York and London (1986).
Keller, E. F., and L. A. Segel, "Traveling Bands of Chemotactic Bacteria: A Theoretical Analysis," *J. Theor. Biol.*, **30**, 235 (1971).
Kennedy, M. J., and J. G. Lawless, "Role of Chemotaxis in the Ecology of Denitrifiers," *Appl. Env. Microbiol.*, **49**, 109 (1985).
Larsen, S. H., R. W. Reader, E. N. Kort, W.-W. Tso, and J. Adler, "Change in Direction of Flagellar Rotation is the Basis of the Chemotactic Response in *Escherichia coli*," *Nature*, London, **249**, 74 (1974).
Lazlo, D. J., and B. L. Taylor, "Aerotaxis in *Salmonella typhimurium*: Role of Electron Transport," *J. Bacteriol.*, **145**, 990 (1981).
Longsworth, L. G., "Tests of Flowing Junction Diffusion Cells with Interference Methods," *Rev. Sci. Inst.*, **21**, 24 (1950).
Lovely, P., F. W. Dahlquist, R. M. Macnab, and D. E. Koshland, Jr., "An Instrument for Recording the Motions of Microorganisms in Chemical Gradients," *Rev. Sci. Instrum.*, **45**, 683 (1974).

Lowe, G., M. Meister, and H. C. Berg, "Rapid Rotation of Flagellar Bundles in Swimming Bacteria," *Nature* (London), **325**, 637 (1987).
Macnab, R. M., "Chemotaxis in Bacteria," *Encyclopedia of Plant Physiology*, W. Haupt and M. E. Feinleib, eds., Vol. 7, Springer-Verlag, Berlin, p. 310 (1979).
Macnab, R. M., and D. E. Koshland, Jr., "The Gradient-sensing Mechanism in Bacterial Chemotaxis," *Proc. Nat. Acad. Sci. USA*, **69**, 2509 (1972).
Macnab, R. M., and M. K. Ornston, "Normal-to-Curly Flagellar Transitions and their Role in Bacterial Tumbling. Stabilization of an Alternative Quaternary Structure by Mechanical Force," *J. Mol. Biol.*, **112**, 1 (1977).
Maeda, K., Y. Imae, J. Shioi, and O. Fumio, "Effect of Temperature on Motility and Chemotaxis of Escherichia coli," *J. Bacteriol.*, **127**, 1039 (1976).
Mesibov, R., G. W. Ordal, and J. Adler, "The Range of Attractant Concentrations for Bacterial Chemotaxis and the Threshold and Size of Response over this Range. Weber Law and Related Phenomena," *J. Gen. Physiol.*, **62**, 203 (1973).
Miller, J. B., and D. E. Koshland, Jr., "Membrane Fluidity and Chemotaxis: Effects of Temperature and Membrane Lipid Composition on the Swimming Behavior of *Salmonella typhimurium and Escherichia coli*," *J. Mol. Biol.*, **111**, 183 (1977).
Nossal, R., and S. H. Chen, "Effects of Chemoattractants on the Motility of *Escherichia coli*," *Nature New Biology*, London, **244**, 253 (1973).
O'Brien, E. J., and P. M. Bennett, "Structure of Straight Flagella from a Mutant *Salmonella*," *J. Mol. Biol.*, **70**, 133 (1972).
Othmer, H. G., S. R. Dunbar, and W. Alt, "Models of Dispersal in Biological Systems," *J. Math. Biol.*, **26**, 263 (1988).
Phillips, B. R., "The Random Movement of Swimming Bacteria: I. Measurements on Individual Cells Compared to Cell-Populations; II. Simulations of Hindered Motility in Small Pores," PhD Thesis, University of Pennsylvania (1992).
Phillips, B. R., and J. A. Quinn, "The Random Movement of Swimming Bacteria: Simulations of Hindered Motility in Small Pores," in preparation (1994).
Poole, P. S., D. R. Sinclair, and J. P. Armitage, "Real Time Computer Tracking of Free-Swimming and Tethered Rotating Cells," *Analytical Biochem.*, **175**, 52 (1988).
Rivero-Hudec, M., and D. A. Lauffenburger, "Quantification of Bacterial Chemotaxis by Measurement of Model Parameters Using the Capillary Assay," *Biotech. Bioeng.*, **28**, 1178 (1986).
Rivero, M. A., H. M. Buettner, R. T. Tranquillo, and D. A. Lauffenburger, "Transport Models for Chemotactic Cell-Populations Based on Individual Cell Behavior," *Chem. Eng. Sci.*, **44**, 2881 (1989).
Ross, S. M., *Introduction to Probability Models*, 3rd ed., Academic Press, Inc., San Diego, CA (1985).
Schlichting, H., *Boundary-Layer Theory*, McGraw-Hill, New York (1979).
Schneider, W. R., and R. N. Doetsch, "Velocity Measurements of Motile Bacteria by Use of a Videotape Recording Technique," *Appl. Microbiol.*, **27**, 283 (1974).
Schneider, W. R., and R. N. Doetsch, "Effect of Viscosity on Bacterial Motility," *J. Bact.*, **117**, 696 (1974).
Segel, L. A., I. Chet, and Y. Henis, "A Simple Quantitative Assay for Bacterial Motility," *J. Gen. Microbiol.*, **98**, 329 (1977).
Segel, L. A., and J. L. Jackson, "Theoretical Analysis of Chemotactic Movement in Bacteria," *Mechanochem. and Cell Motility*, **2**, 25 (1973).
Shioi, J., C. V. Dang, and B. L. Taylor, "Oxygen as Attractant and Repellent in Bacterial Chemotaxis," *J. Bacteriol.*, **169**, 3118 (1987).
Silverman, M., and M. Simon, "Flagellar Rotation and the Mechanism of Bacterial Motility," *Nature*, London, **249**, 73 (1974).
Staffeld, P. O., and J. A. Quinn, "Diffusion-Induced Banding of Colloidal Particles via Diffusiophoresis," *J. Colloid Interface Sci.*, **130**, 69 (1989).
Stanton, T. B., and D. C. Savage, "Colonization of Gnotobiotic Mice by *Roseburia cecicola*, a Motile, Obligately Anaerobic Bacterium from Murine Ceca," **45**, 1677 (1983).
Taylor, B. L., and D. E. Koshland, Jr., "Intrinsic and Extrinsic Light Responses of *Salmonella typhimurium and Escherichia coli*," *J. Bacteriol.*, **123**, 557 (1975).
Tsang, N., R. M. Macnab, and D. E. Koshland, Jr., "Common Mechanism for Repellents and Attractants in Bacterial Chemotaxis," *Science*, **181**, 60 (1973).

Appendix

The models of Othmer et al. (1988) and Rivero et al. (1989) assume that the tumbling response is the result of a Poisson process. We measure the time between tumbles—the run length times. The following analysis shows how the tumbling probability can be determined from these measurements of run length times (Ross, 1985).

Begin by assuming that we are following one cell starting at time zero. If $N_P(t)$ represents the total number of tumbles which have occurred up to time t, then $N_P(t)$ is a Poisson process if the following requirements are met:

(i) $N_P(0)=0$

(ii) The process has stationary and independent increments

(iii) The number of tumbles in any interval of length t is Poisson distributed with mean $\lambda_T t$ (standard deviation $\sqrt{\lambda_T t}$). For all times, a, $t \geq 0$,

$$P\{N_P(t+a)-N_P(a)=n\}=\frac{(\lambda_T t)^n \exp^{-\lambda_T t}}{n!}, \qquad n=0, 1, 2, \ldots \quad \text{(A1)}$$

Definition (i) simply means that only those tumbles are counted which occur at time $t>0$. From definition (ii), a process is said to have independent increments if the numbers of events which occur in disjoint time intervals are independent. The definition of stationary increments is satisfied if the distribution of the number of tumbles which occur in any interval of time is dependent only on the length of the time interval. The process rate intensity, or in this case the tumbling probability, λ_T, is defined by Eq. A2:

$$\lim_{\Delta t \to 0} \left\{ \frac{\text{Probability (exactly one event in } [t,\ t+\Delta t])}{\Delta t} \right\} = \lambda_T \quad \text{(A2)}$$

Equation A1 therefore determines the probability that n tumbles occur in the time interval (a, t).

The probability that zero tumbles occur in time $(0, t)$ is equal to the probability that the first run length time, T_1, is greater than t. From Eq. A1, this probability is given by:

$$P\{N_P(t)=0\}=P\{T_1>t\}=\frac{(\lambda_T t)^0 \exp^{-\lambda_T t}}{0!}=\exp^{-\lambda_T t} \quad \text{(A3)}$$

Since the probability that T_1 occurs between times $(0, +\infty)$ is one, then the cumulative probability, or the probability that T_1 is less than or equal to t is given by Eq. A4:

$$P\{T_1 \leq t\}=1-P\{T_1>t\}=1-\exp^{-\lambda_T t} \quad \text{(A4)}$$

Equation A4 is the cumulative probability of an exponential process. The probability density function of a random variable is the derivative of the cumulative distribution. Taking the derivative of Eq. A4, the probability that the run length time

T_1 is equal to some time t is defined by the exponential probability function:

$$P(T_1 = t) = \lambda_T \exp^{-\lambda_T t} \tag{A5}$$

The mean and standard deviation of an exponential process are both given by λ_T^{-1}. Therefore, the run length time, T_1, is exponentially distributed with mean λ_T^{-1}. This same approach can be used to show that the entire sequence $\{T_n, n = 1, 2, \ldots\}$ is exponentially distributed with mean λ_T^{-1}. Thus, if the tumbling rate is the result of a Poisson process with rate intensity λ_T, then the time between tumbles or the run length time is exponentially distributed with mean and standard deviation λ_T^{-1}.

The analysis above is for an individual cell. In the experiments conducted here, we are measuring the run length times for many different cells. Therefore, an underlying assumption of this approach is that all cells in the population exhibit the same random motility. This assumption is also present in the population studies where the dispersion of a cell-population is modeled with a single random motility coefficient, μ. Brown (1974) found both cell speed and turn angle (index of directional persistence) to be uniform from cell-to-cell within a given population. He also determined that the mean run length times of individual cells within a cell-population were lognormally distributed. The mean ($\pm$standard deviation of the mean) of the mean run length times of 34 cells was determined to be 1.2 ± 0.3 s. Due to the relatively small standard deviation of this mean run length time distribution as compared to about 1.2 s standard deviation for each individual cell, the assumption that all cells exhibit the same random motility can be considered valid. Randomly measuring a single run length time from many cells is then equivalent to measuring many run length times from an individual cell. Because a cell's run length time is independent of whether or not the cell is swimming within the plane of focus, the cell run length times measured represent a random sampling.

As stated above, the measured run length times are expected to be exponentially distributed. From these run length times the tumbling probability, λ_T, is determined by two methods. The first is simply from the arithmetic mean. The second method is obtained by rearranging Eq. A3. Taking the natural logarithm of both sides of Eq. A3 gives:

$$\ln(g) = -\lambda_T t \tag{A6}$$

where g represents the fraction of runs of length greater than t. From Eq. A6, the tumbling probability or reciprocal persistence, λ_T, can be obtained from the slope of the plot of $\ln(g)$ vs. t. The standard deviation of the lefthand side of Eq. A6 is given by (Blanc-Lapierre and Fortet, 1965):

$$\sigma_{\ln(g)} = \sqrt{\frac{1-g}{N_R g}} \tag{A7}$$

where N_R is the total number of runs measured.

Manuscript received July 31, 1992, and revision received June 30, 1993.